Phys. Med. Biol. 40 (1995) 181–199. Printed in the UK

A Monte Carlo investigation of dual-energy-window scatter correction for volume-of-interest quantification in $^{99}Tc^{m}$ SPECT

Jian-qiao Luo†, Kenneth F Koral†, Michael Ljungberg‡, Carey E Floyd Jr§ and Ronald J Jaszczak§

† Division of Nuclear Medicine, Department of Internal Medicine, University of Michigan Medical Center, Ann Arbor, MI, USA

‡ Department of Radiation Physics, University of Lund, Lund, Sweden

§ Department of Radiology, Duke University Medical Center, Durham, NC, USA

Received 1 February 1994, in final form 9 September 1994

Abstract. Using Monte Carlo simulation of $^{99}Tc^{m}$ single-photon-emission computed tomography (SPECT), we investigate the effects of tissue-background activity, tumour location, patient size, uncertainty of energy windows, and definition of tumour region on the accuracy of quantification. The dual-energy-window method of correction for Compton scattering is employed and the multiplier which yields correct activity for the VOI as a whole calculated. The model is usually a sphere containing radioactive water located within a cylinder filled with a more dilute solution of radioactivity. Two simulation codes are employed. Reconstruction is by ML–EM algorithm with attenuation compensation. The scatter multiplier depends only slightly on the sphere location or the cylinder diameter. It also depends little on whether correction is before or after reconstruction. At low background level, it changes with VOI size, but not at higher background. For a geometrical VOI, it is 1.25 at zero background, decreases sharply to 0.56 for equal concentrations, and is 0.44 when the background concentration is very large. Quantification is accurate (less than 9% error) if the test background is reasonably close to that used in setting the universal scatter-multiplier value, or if the test backgrounds are always large and so is the universal-value background, but not if the test backgrounds cover a large range of values including zero. Results largely agree with those from experiment after the experimental data with background is re-evaluated with prejudice.

1. Introduction

A nuclear-medicine gamma camera has a finite energy resolution due to its construction. To accumulate most of the emitted photons which have not undergone scattering in the patient, the main acceptance window (alias photopeak window) must therefore have a finite width. Due to this finite width, however, the accepted data will include counts from photons which have undergone Compton scattering and lost some energy before detection. Such included counts will be distributed throughout the projection image. For regions of the image which are important to focal quantification, there will be counts added beyond those consistent with the true source activity, given a model of attenuation effects based on total cross-sections. When reconstructed with attenuation correction, these counts will erroneously increase apparent source activity. This fact was well shown for a non-radioactive volume by Jaszczak (Jaszczak *et al* 1984), but is true for radioactive volumes as well. The latter volumes are of interest in heart studies and radiopharmaceutical therapies. The magnitude of the problem for focal quantification depends on how far away and how strong confounding activities are, and on what type of calibration is used to convert reconstructed counts to measured activity.

0031-9155/95/010181+19$19.50

A number of scatter compensation techniques (Devito *et al* 1989, Gagnon *et al* 1989, Gilardi *et al* 1988, Jaszczak *et al* 1984, King *et al* 1992, Koral *et al* 1988, Ljungberg and Strand 1990b, Ogawa *et al* 1991, Wang and Koral 1992, Yanch *et al* 1990) have been developed for use with gamma cameras. The dual-energy-window (alias, scatter-multiplier) method (Jaszczak *et al* 1984) has the advantages of simplicity and ease of application. For SPECT, it is based on dual-energy-window tomographic data acquisition, which is now widely available, and has two possible modes: subtracted projections (SP) and subtracted tomograms (ST) (Koral *et al* 1990). For all applications known to us, a single 'universal' value of the scatter multiplier, k, is used for all projections (SP mode) or for all transverse planes (ST mode).

In SP mode, a sufficient condition for correction success is that, for every pixel in every projection, the number of scattered photons detected in the photopeak window is proportional to the number of photons detected in the secondary, lower-energy (scatter) window. Then, the scattered photons in the photopeak window can be estimated by the scatter multiplier multiplied by the counts in the scatter window and can be subtracted. Thus, a projection can potentially be corrected and, when all projections are corrected, the resulting reconstruction should be accurate.

Unfortunately, it is already known that a single value of k does not exist for all pixels in a projection image (Ljungberg and Strand 1990a). Thus, the sufficient condition for correction is not met for even one projection, yet alone all.

A necessary condition for correction success in a volume of interest (VOI), however, can be defined for both modes. The necessary condition is that the net reconstructed count for the corrected data is the same as that for reconstruction of only the unscattered component of the data.

Experimentally, the k for a radioactive $^{99}Tc^{m}$ sphere located in a non-radioactive or radioactive cylinder has already been measured (Koral *et al* 1990; this reference will be called the experimental reference hereafter). It was found to be approximately constant as a function of cylinder diameter, hot-sphere location and level of cylinder activity (alias background). With Monte Carlo, scattered photons can be tagged and effects from them determined, while with an experiment, such tagging is impossible. The technique employed experimentally for choosing k (Jaszczak *et al* 1984, experimental reference) is indirect but reasonable: it is assumed that accurately estimating counts or activity for an object in a complex phantom, relative to a scatter-free phantom, implies scatter correction has been achieved.

The purpose of the present research is to use Monte Carlo simulation to investigate VOI quantification of radioactive structures and the effect on that quantification of dual-energy-window scatter correction. We will find the k that satisfies the necessary condition stated above for each of a variety of phantom geometries. By so doing, we will check the previous experimental results, extend the parameter variation and look at new parameters. We will not consider phantoms which have non-uniform attenuation nor investigate the effects of statistical noise. We will not try to optimize the window widths or locations. Nor will we look at a smaller target sphere where resolution effects will dominate scatter effects; we expect recovery coefficients must be included for those cases, as we have recently done clinically with ^{131}I (Koral *et al* 1994). Moreover, these recovery coefficients probably have at least some background dependence so this more general quantification case requires further study. $^{99}Tc^{m}$ will be the radioisotope investigated here, but isotopes such as ^{131}I may follow the same trends.

2. Method

2.1. Monte Carlo codes

Two Monte Carlo simulation packages are employed. They are the MC code developed by John Beck and one of the authers (CF) at Duke University (Beck 1982, Floyd *et al* 1984) and the SIMIND code written by one of the authors (ML) at the University of Lund, Sweden (Ljungberg and Strand 1989). We modified the original codes to include multiple energy windows for projection images. We use the MC code for most simulations, but we verified in several cases that the SIMIND code gave essentially the same results. Object activity is specified by inputing the total for MC and the concentration for SIMIND. Both simulation packages are installed on a Stardent computer. It is connected to a local network which contains UNIX/ULTRIX-based workstations, VMS-based computers, and Macintosh computers, all of which are used in our data analysis.

We want to investigate the basic dependence of k on geometric parameters without complications from the effects of noise. By definition, a photon history is a record of the interactions and path which are particular to a single photon's life time (Raeside 1976, Andreo 1991). We use of the order of a few million (sometimes) up to hundreds of millions (usually) of histories for the individual simulations. Since the statistical noise of an image is inversely related to the number of histories, these large numbers make the total counts within a large spherical VOI almost statistically noise free. Photons are allowed to undergo up to six orders of scattering. The majority of photon scattering of interest is first and second order. The attenuation medium is 'soft-tissue equivalent' or simply water.

2.2. Phantom

The basic phantom object for the Monte Carlo study duplicates one that is commercially available for experimental studies and which was used in the experimental reference. It is a cylinder, 20.5 cm in diameter and 23.8 cm long. It usually contains one uniform sphere, 5.65 cm diameter, which is located midway along the cylinder length and either on axis (see figure 1) or 5.7 cm off axis. Filled with radioactive or non-radioactive water, the sphere represents a tumour or an organ and the cylinder the tissue of the rest of the body.

To investigate the effects of different body size, which is a variable in any group of patients, three phantoms, having the cylinder diameter (1) standard, (2) reduced to 15 cm, and (3) expanded to 25 cm, are simulated. For these simulations, the sphere is on axis and there is no background activity. To investigate the dependence of the scatter multiplier on the location of the target source, which also varies for patients, we calculate k values for the two sphere positions within the standard cylinder at two different levels of activity outside the sphere ('tissue'-background activity). The background level is defined by the ratio of activity concentration in the cylinder over that in the sphere. That is, the background ratio, b, is given by

$$b = A_{\mathrm{cyl}} V_{\mathrm{sph}} / [A_{\mathrm{sph}} (V_{\mathrm{cyl}} - V_{\mathrm{sph}})] \qquad (1)$$

where A_{cyl} is the total activity in the cylinder exclusive of the sphere, A_{sph} is the total activity in the sphere, and V_{cyl} and V_{sph} are the volume of the cylinder and the volume of the sphere respectively. The tested b values are 0.0 and 0.2.

To look more generally at the consequences of background activity, two types of distribution are studied:

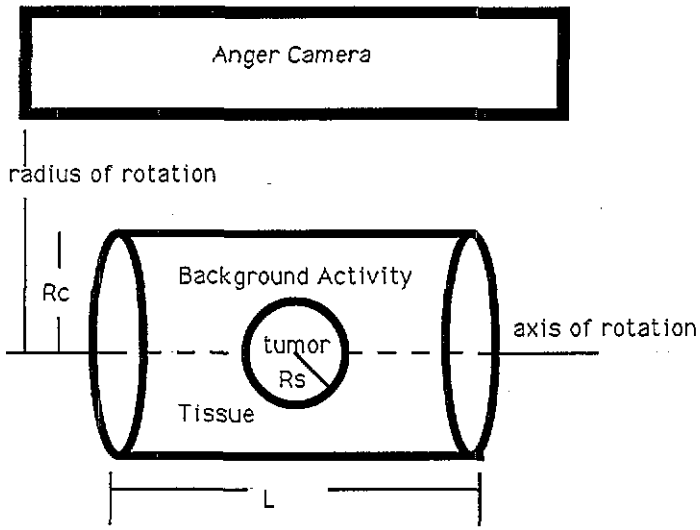

Figure 1. A simulated phantom that consists of one uniform-activity sphere located on the axis of a cylinder with uniform background activity. The camera rotates around the phantom for tomographic data acquisition.

(1) The first involves a uniform background throughout the standard cylinder with a radioactive sphere on or aff axis, as above. The different b values are $b = 0$ for a hot sphere in a cold cylinder $b = 0.1$, 0.2, 0.5 for a hot sphere in a warm cylinder, and $b = 1.0$ for a hot sphere in an equally hot cylinder.

(2) The second involves a non-uniform background but is for only the off-axis location of the target sphere. Three other spheres are located 5.7 cm off the axis of the standard cylinder so the four are arranged symmetrically. The three are identical to each other as concerns activity and, together with the part of the cylinder which is free of activity, form the non-uniform background for the target sphere. The ratio of the activity concentration in each of the three spheres over that in the target sphere is 5.5 which makes the average concentration in the volume outside the target sphere over the concentration in the target sphere equal to 0.2.

2.3. Anger camera

In both Monte Carlo codes, a low-energy, general-purpose, parallel-hole Anger-camera collimator is simulated. The collimator hole is circular for MC and hexagonal for SIMIND and has a size of about 0.25 cm and a length of about 4.0 cm. An effective collimator thickness is calculated within the programs to account for collimator penetration.

The energy-output signal for each detected photon is sampled from a camera energy-resolution function (a Gaussian distribution is assumed). The FWHM is proportional to the square root of the gamma-ray energy (Knoll 1979). The energy resolution of the camera is 10.8% at 140 keV. Camera-output signals are originally assigned to 2 keV wide energy channels. Therefore, energy spectra are available for inspection and analysis. Final data sets are obtained by summing specified channels to simulate wider windows.

Spatial resolution R_s of the SPECT system is determined by the collimator resolution R_c and the intrinsic detector resolution R_i. In the MC code, R_c for a parallel-hole collimator is

written as

$$R_c = a(L + d - Z)/L. \tag{2}$$

Here, d is the distance between the collimator face and the axis of rotation, Z is the signed distance from the last scattering site to the axis of rotation, a is the hole diameter, and L is the hole length. R_i is specified by an input parameter and added in quadrature to R_c to obtain R_s. The apparent point of detection is found from the detector intersection point modified by sampling a Gaussian whose FWHM is specified by R_s. In the SIMIND code, each photon is emitted or scattered into a maximum solid angle that is dependent on the collimator thickness and hole size. When the photon enters a hole, a geometrical test is made as to whether or not the photon passes through the hole without striking the sides. If not, the photon is rejected and a retry within the solid angle is made. Included is the actual shape of the hole. This rejection technique will give the collimator resolution R_c. The resultant detector-plane location is modified by sampling an energy-dependent Gaussian whose FWHM is governed by the input parameter, R_i.

For $^{99}Tc^m$, a 20% photopeak window is used in clinical applications. Thus, usually for our studies, the photopeak energy window starts at 126 keV and ends at 154 keV, and we choose the scatter energy window to start at 98 keV and end at 126 keV. In addition to the separation due to the two separate energy windows, the simulated data are further separated into two components for each window: a scatter-free (alias direct, primary, or unscattered) component for the photons that reach the detector without undergoing any scattering and a scatter component for the photons that are scattered at least once. The four final different components are given labels in figure 2. Any photon with energy-output signal below 98 keV or above 154 keV is eliminated from further consideration.

It has been noted that, with the split-photopeak method for Compton-scatter correction, energy windows which shift between calibration and the measurement to be corrected cause a large problem (King *et al* 1992). Such shifts can occur because of electronic drift or setting mistakes. As a special study, we examine the effects of a large upward shift of 6 keV for both windows, in the case of the on-axis sphere in the standard cylinder with $b = 0.0$ and 0.2. We calculate the percentage error in the activity from using the k which is correct for the unshifted window.

2.4. *Tomographic acquisition and reconstruction*

The distance between the cylinder axis, which is the centre of rotation for the tomographic acquisition, and the front face of the camera is chosen to be 15.0 cm. When the sphere is located on axis, a whole projection set, which includes 64 angles, is simply multiple copies of the same simulated projection since the view from all angles is identical. When the phantom is non-symmetrical, we generate a set of 64 appropriate projection images. Image resolution of all simulations is 64×64 pixels to reduce both simulation time and also required data storage. The value of the attenuation coefficient is 0.151 cm^{-1}.

Tomographic images are reconstructed by the ML–EM algorithm with attenuation correction (Shepp and Vardi 1982, Gullberg *et al* 1985). The attenuation maps are produced by a geometric function since the attenuating object has a cylindrical shape.

The number of iterations in the ML–EM reconstruction is chosen to be 16. In general, the appropriate number of iterations will depend upon the details of object geometry, uniformity of the attenuating medium, and camera resolution. We are interested in the quantification of a SPECT image for a relatively large volume (94.34 cm^3 for the sphere). Therefore, we only want to ensure that the ML–EM reconstruction converges for this specific volume of

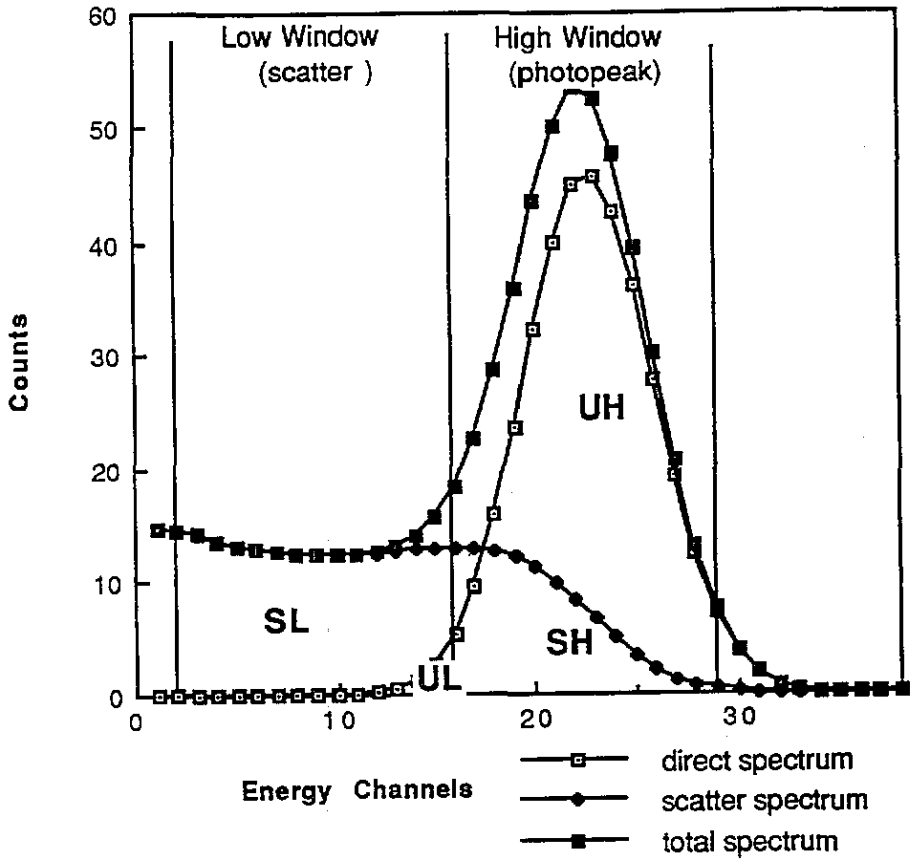

Figure 2. Energy spectra from the entire projection image for a hot sphere in a cylindrical phantom with background ($b = 0.2$). The separation into scattered and scatter-free components, which is possible with Monte Carlo simulation, as well as the total (sum), are shown. Energy windows and the labels for each component within each window (UH for unscattered in high window, UL for unscattered in low window, SH for scattered in high window, and SL for scattered in low window) are indicated.

interest and for our relatively simple geometry. The effect of the number of iterations on the reconstructed count within a volume of interest has been tested for experimental data using SP mode and $k = 0.75$. The number of iterations took on the value of one, two, four, eight, 16, up to 32. The reconstructed VOI count increased rapidly with the number of iterations when the number was below four and approached a constant after eight iterations. Similar results are obtained from the ML–EM reconstructions for our Monte Carlo simulated data. Therefore, it is safe to choose 16 iterations.

2.5. Data analysis

The counts within a spherical VOI are of interest to us. A set of circles with radii defined by r_i

$$r_i = \sqrt{R_s^2 - d_i^2} \tag{3}$$

specifies the boundary. Here, R_s is the radius of the sphere and d_i is the distance from the ith to the centre slice. The k value needed to remove the effect of scatter may vary with the VOI size employed. Therefore, besides the standard geometric-size VOI, we test VOIs which have half, twice, and four times the diameter of the standard. The phantom is an on-axis sphere in the standard cylinder with $b = 0.0$, 0.2, 0.5, and 1.0. We also repeat the test for the off-axis sphere.

For a given VOI, the method for calculating the k value depends on the correction mode. In ST mode, k is obtained directly from the following equation:

$$k = C_{SH}/(C_{UL} + C_{SL}) \tag{4}$$

where C_{SL}, C_{UL} and C_{SH} are the VOI counts from the reconstructions for components SL, UL and SH defined in figure 2. This equation follows from our stated necessary condition for k and an assumption of linearity over components for the reconstruction algorithm. That is, we assumed, for example, that the count from reconstructing UH plus the count from reconstructing SH was equal to the count from reconstructing UH plus SH. The assumption was checked in an individual case. The reconstructed-count-weighted average of the absolute value of the error was less than 0.2%.

In SP mode, (1) two trial values of k are chosen, (2) error values are calculated for each, and (3) a final k value is chosen as that which gives zero error according to linear interpolation. This idea is explained in the experimental reference. The exact details of its implementation for our Monte Carlo simulations are stated by Luo (1993).

In ST mode, a closed-form equation to estimate the k value for any uniform background in terms of several calculated parameters is available (Luo 1993):

$$k = \frac{d_s N_1 + d_c N_2 (V_{cyl}/V_{sph}) b}{(b_s + c_s) N_1 + (b_c + c_c) N_2 (V_{cyl}/V_{sph}) b}. \tag{5}$$

Here, six unknown coefficients, b_s, b_c, c_s, c_c, d_s, and d_c, are first to be determined by two simulations which have different b values. N_1 and N_2 are the total number of histories for the first and the second simulation respectively. This equation depends on taking a formulation which is rigorously correct for a single projection and applying it to a set of reconstructed images. To test the accuracy of so doing, we calibrate the equation twice with different pairs of b values and compare the results to each other. The calibration pairs are $b = 0$, $b = 1$ and $b = 0.2$, $b = 1$. We also evaluate how close each result at a non-calibration b value is to the result from equation (4).

2.6. *Quantification error in the face of background*

Target activity is calculated from the net counts within a VOI. Assuming there is no error in the camera calibration constant, the percentage error in the activity, ε, is equal to the percentage error in this net count.

When no scatter correction is employed, ε can be shown to be given by the ratio of reconstructed counts from component SH to those from UH:

$$\varepsilon = C_{SH}/C_{UH}. \tag{6}$$

We evaluate activity error using equation (6) for the specific cases of a sphere on or off axis in a standard cylinder with a specified background.

With scatter-multiplier correction for a VOI,

$$C_{SC} = C_P - kC_S \tag{7}$$

where C_{SC} is the scatter-corrected reconstructed count, C_S is the reconstructed count for the scatter-window data, and C_P the reconstructed count for the photopeak window data (Jaszczak *et al* 1984). The final estimate of corrected activity with k-value correction is now directly proportional to C_{SC}. Therefore, the percentage error in activity is calculated from the percentage error in C_{SC}. We examine the activity error for the specific cases of a sphere (1) on or off axis in a specified cylindrical background when the no-background, off-axis k value is employed universally and (2) in a specified uniform background with windows shifted, when the unshifted-windows k value is employed. In both cases, the percentage error in activity, ε_k, by the arguement above, is given by

$$\varepsilon_k = (C_{SC} - C_T)/C_T \tag{8}$$

where C_T is the true unscattered reconstructed count within a spherical VOI and C_{SC} is the scatter-corrected result under either of the two procedures specified above.

A possible alternative in quantification would be to ignore scatter correction and employ a scatter-included phantom for the camera calibration. We investigate the accuracy of this technique for the Monte Carlo simulations of the hot sphere on and also off axis, again as a function of background. We take the result for the on-axis sphere with no background as the calibration experiment. That is, the calibration constant with no explicit scatter correction, e_{nsc}, is given by

$$e_{nsc} = (C_{UH} + C_{SH})/N \tag{9}$$

where C_{UH} and C_{SH} are reconstructed VOI counts at $b = 0$ for components UH and SH respectively and N is the total number of histories. For the test cases, the calculated activity, A, is given by

$$A = [C_{UH}(b) + C_{SH}(b)]/e_{nsc} \tag{10}$$

where $C_{UH}(b)$ and $C_{SH}(b)$ are reconstructed VOI counts at $b \neq 0$. The true activity, A_T, can be shown to be (Luo 1993)

$$A_T = NV_{sph}/[b(V_{cyl} - V_{sph}) + V_{sph}]. \tag{11}$$

The error, ε_P, is now given by an equation analogous to equation (8) but with ε_P replacing ε_k, A replacing C_{SC}, and A_T replacing C_T.

2.7. Re-evaluation of experimental phantom data

As will be shown in the results, the dependence of k on background level is not the same for the Monte Carlo results as it is for the originally published experimental results (experimental reference). We therefore undertake a limited re-evaluation of that experimental data. A subset (the rest of the data were lost or could not be retrieved from archival tapes) of it is available to us for re-evaluation. Tomographic data sets for the sphere off axis with cylinder background at five values including zero, all taken on the same day, are available. Two other zero-background data sets taken a day earlier and the camera-calibration data set are not.

We choose not to approximate a $b = 1.0$ datum by moving the sphere volume of interest axially to a part of the cylinder containing background as had been done before. The ML–EM reconstruction algorithm is our latest version. The dead-time corrections are re-evaluated using a newly available method (Zasadny *et al* 1993). That is, we employ a separate correction for the data in each window; both corrections are based on a paralysable model but with different constants. To locate the sphere VOI more accurately, we scan the volume of specified size over the three-dimensional volume of reconstructed photopeak-window data looking for the location that gives maximum counts. The value so determined is divided by true sphere activity to yield what we call specific reconstructed counts within the sphere. The same location is used for both windows. Since the experimental estimation of scale value can have some error, we evaluate results for the nominally correct size and for larger and smaller values as well.

It can be shown that the specific reconstructed count within the sphere is linearly related to the experimental b value (Luo 1993). This relation was looked for in figure 3 of the experimental reference and is sought again in this re-evaluation. In terms of the slope, β, and intercept, α, for the linear relationship for the photopeak window (subscript p) and scatter window (subscript s), the scatter multiplier can also be shown (Luo 1993) to be given by

$$k = (\alpha_p + \beta_p b - e_{sc})/(\alpha_s + \beta_s b) \tag{12}$$

where e_{sc} is the camera calibration constant needed for quantification with scatter correction. Since no experimental calibration data are available for re-evaluation, we allow e_{sc} to vary: for a given-size VOI, it is set by requiring agreement between the experimental and Monte Carlo k values at $b = 0$. Making this choice also affects the slope, dk/db at $b = 0$, however. This procedure is followed as a consistency test between the experimental and Monte Carlo data when the experimental calibration constant is unknown (one can say the experimental data are being re-evaluated with prejudice). If the procedure leads us to a calibration constant that is significantly in error for the experiment, then conclusions about the experimental data are incorrect. A careful re-execution of the experiment is needed to reveal such an error.

3. Results

All results in this section are from ST mode unless specified otherwise.

3.1. Effect of phantom size

We plot the k value against cylinder diameter in figure 3. One sees that, at least at this background level, there is very little dependence on diameter. One also sees that the correction mode changes the magnitude of the k value slightly, but does not affect the near independence of k from diameter. This near independence is in agreement with the SP-mode experimental result (table 2 and/or figure 5 of the experimental reference) although there the diameter range was only 20.5–22.2 cm. The k values with ST mode are slightly larger than in SP mode for both Monte Carlo (figure 3) and experiment (table 2 of the experimental reference).

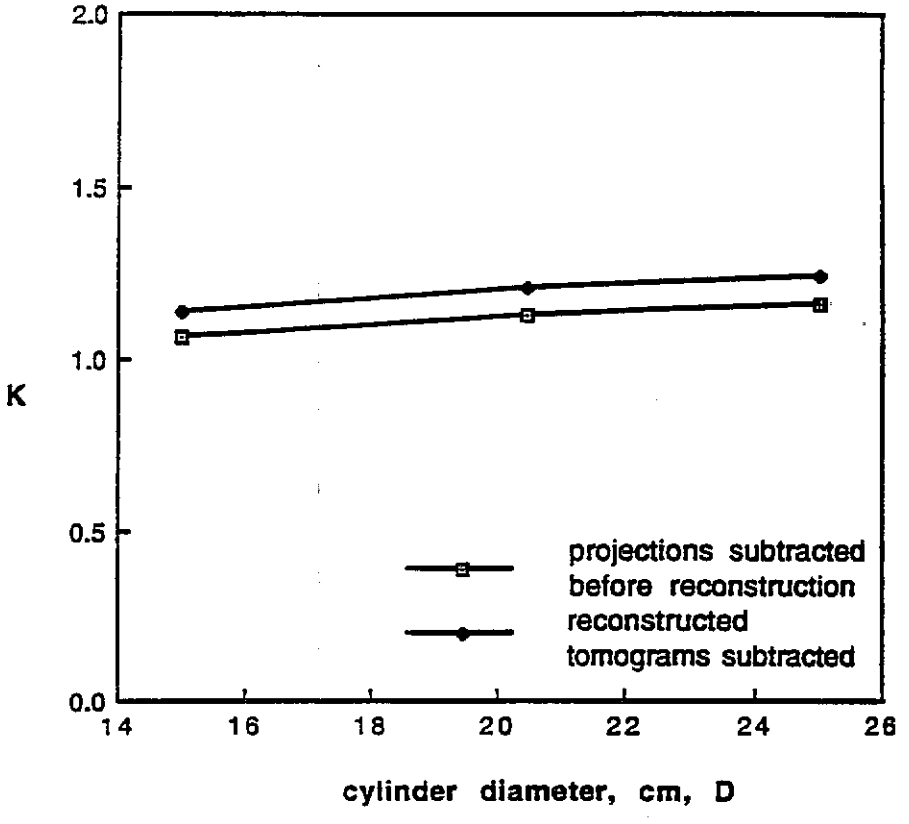

Figure 3. Required k versus cylinder diameter with no cylinder background. Geometric-size VOI (5.65 cm diameter), SP and ST modes.

3.2. Effect of source location

A plot of k value versus radioactive-sphere location with background as a parameter is shown in figure 4. There is very little dependence on source location at either background level. The only experimental test of k dependence on source location, with zero background (figure 5 in the experimental reference), is in qualitative agreement with the $b = 0$ result of figure 4. The Monte Carlo results show a fairly large dependence on background level. This dependence is covered more generally in the next section.

3.3. Effect of background activity

Figure 5 plots energy spectra for the on-axis sphere in a uniform cylinder. The scattered-photon spectrum is shown for two cases: with activity only in (1) the sphere and (2) the cylinder. The spectra are taken from the spheres circular region of interest in a projection. The spectra are normalized so that there is exactly the same number of counts within the usual photopeak window for both. Within the scatter window, the spectral shapes are quite different; the number of counts in that window from the cylinder is much larger than the number from the sphere. When the background parameter b is increased, the cylinder spectrum will increasingly dominate the total scattered-photon spectrum and the relative number of counts in the scatter window will increase. The scatter multiplier needed for

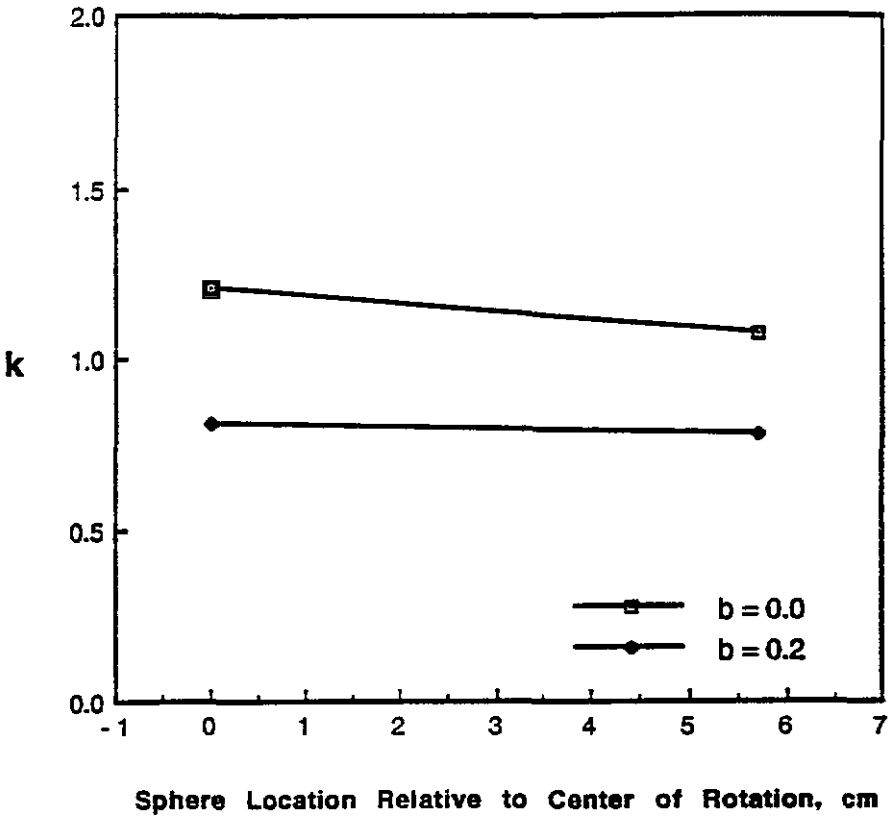

Figure 4. Required k versus source locations with the ratio of background activity concentration (cylinder divided by sphere), b, as a parameter. Geometric-size VOI (5.65 cm diameter), standard-size cylinder, ST mode.

correction, therefore, is expected to decrease. This decrease is found in our calculated results. A typical dependence of k on background is shown in figure 6. The scatter multiplier starts at 1.05 at $b = 0$ but decreases rapidly as background increases. It then slows its decrease and levels off as b approaches 1.0. This result is in disagreement with the constancy reported from experiment (figure 4 of the experimental reference).

For the non-uniform distribution of background activity, the scatter multiplier is calculated as 0.780. Compared with the scatter multiplier (0.778) for uniform background at $b = 0.2$, the difference is less than 3%. From this limited test, we infer that whether the tissue background is uniform or non-uniform but located with approximately the same centroid does not affect the value of the scatter multiplier.

The two calibrations of equation (5) give almost identical curves. These can be found in the dissertation by Luo (1993). Results from the tests against equation (4) are given in table 1 as percentage differences. The small values validate the equation.

Equation (5) allows one to examine k as b approaches infinity, the case of a non-radioactive sphere. While $k = 0.559$ at $b = 1.0$ for the off-axis sphere, it approaches 0.441 as b approaches infinity. This value is similar to the $k = 0.5$ that Jaszczak *et al* (1984) used for qualitative, experimental correction of a non-radioactive sphere.

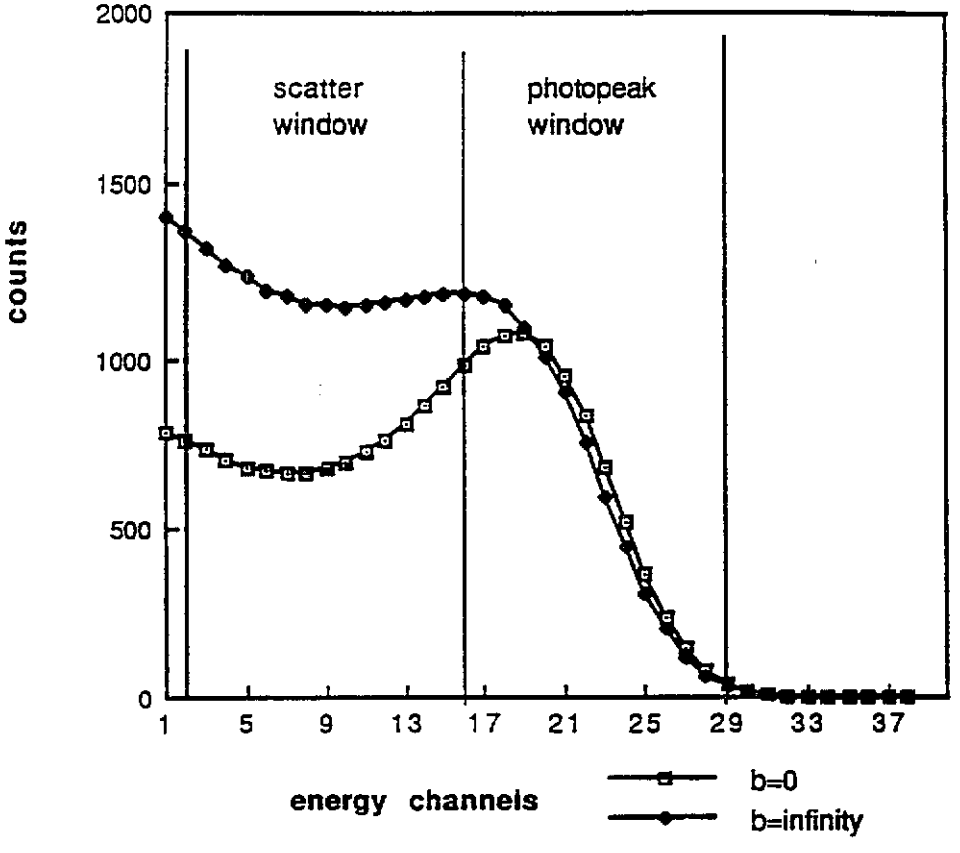

Figure 5. Scatter energy spectra within a region of interest (ROI) for an on-axis hot sphere in a cold cylinder and for an on-axis cold sphere in an hot cylinder. ROI diameters equal to 5.648 cm. Spectra are normalized for equal counts in the photopeak window.

3.4. Effect of VOI size

Figure 7 gives the k value versus VOI size as computed with equation (4). The figure shows that the k value drops rapidly with increasing VOI size when there is no background activity but drops more slowly or is almost constant when the background is large. When $b = 0$, the decrease is similar to that found experimentally under the conditions that the VOI for the photopeak image is kept constant while that for the scatter window increases (Koral *et al* 1991). The equivalent plot for an off-axis sphere can be found in the dissertation by Luo (1993). The results are qualitatively the same.

We note that gross plots of k versus background for a given-size VOI can be made by reading values off the figure along a vertical line. One can thus see that the strong dependence on background decreases as the VOI becomes very large, but this fact is not of practical help because clinical images usually have other structures in the neighbourhood of the VOI which would change this result.

3.5. Quantification error in the face of background

The quantification error with no Compton-scatter correction as a function of background level and distribution is shown in table 2. The positive values indicate the estimate of

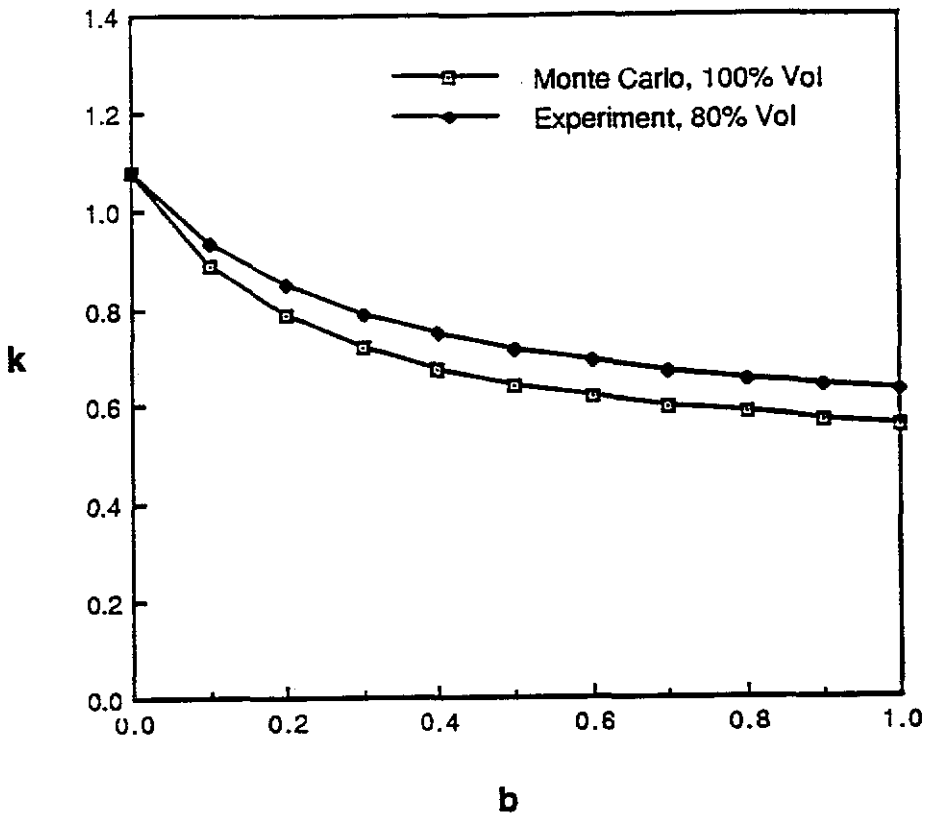

Figure 6. Dependence of scatter multiplier required for quantitative accuracy within radioactive sphere on level of cylinder background. Plot one is a typical Monte Carlo result (geometric vol). Plot two is the result from experiment under the conditions specified in the text. Agreement is good.

Table 1. Scatter multiplier from the pre-calibrated formula compared to that from the definition with the on-axis sphere in uniform background. Two sets of calibrations are tested. Results are from a geometric vol.

Background activity ratio, b		Percentage difference in k from (4) versus that from (5)
For calibration	For evaluation	
0.0, 1.0	0.2	−3.04
0.2, 1.0	0.0	−1.35

activity is too large as expected. The calculated results show the error to be already above 19% at zero background and to increase as the background level increases.

The quantification error from using Compton-scatter correction with a universal k value is given in table 3. The k value chosen is that which is correct for the off-axis sphere in zero background. The errors are mostly negative, indicating overcorrection, but their absolute value is less than 9% as long as the background does not get above $b = 0.2$. With larger background, the error can be quite large.

Table 4 shows that a very large energy shift distorts the calculated activity by no less

than 22%. For the same cases, Luo (1993) shows that with the original split-photopeak correction method, the errors are much larger, being as big as 90%. It appears that the scatter-multiplier method is more stable against energy shifts.

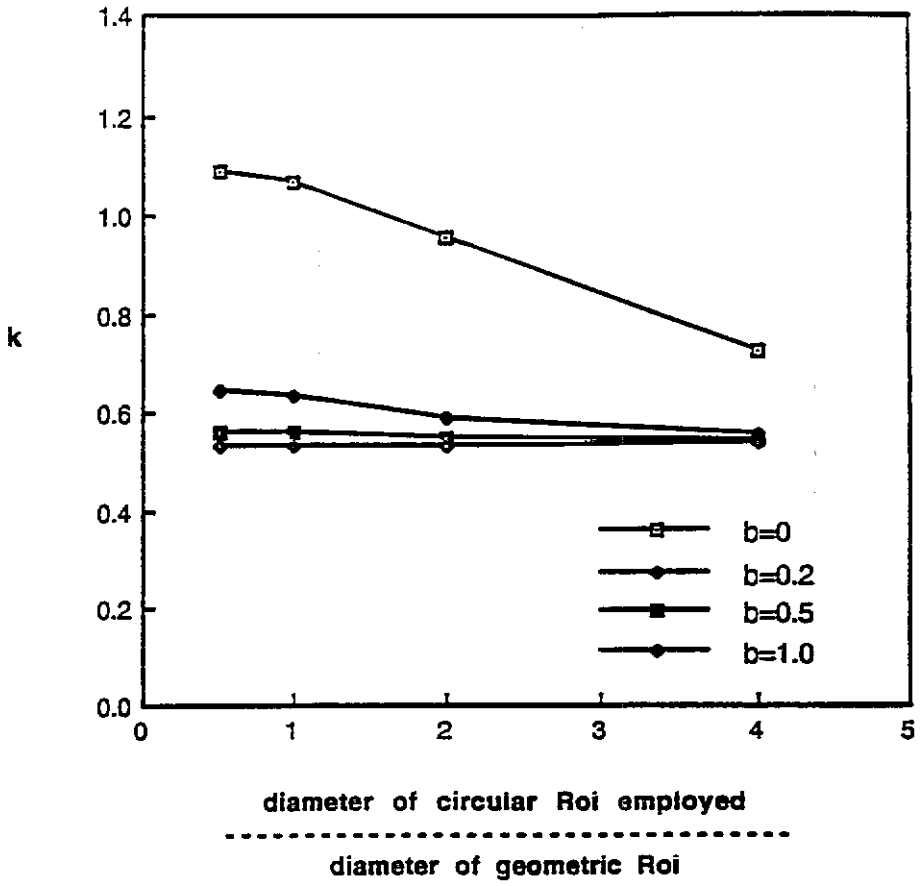

Figure 7. Required k versus VOI size with b as a parameter. The sphere is on axis in a standard cylinder and the VOI size is represented by the ratio of the VOI diameter to the diameter of the geometric VOI. ST mode.

Table 2. Percentage activity error when no correction and a scatter-free camera calibration are employed. Dependence on background and sphere location is given.

Background activity		Hot-sphere location in cylinder	
Type	Ratio, b	On axis	Off axis
Uniform	0.0	19.97	18.22
Uniform	0.2	25.66	22.65
Uniform	0.5	33.47	28.88
Uniform	1.0	41.69	37.84
Non-uniform	0.2	—	24.87

Table 3. Percentage activity error due to background for both on-axis and off-axis cases when using a universal scatter multiplier. That scatter multiplier is determined from the zero-background, off-axis case. Thus the error is zero for that element of the grid.

Background activity		Hot-sphere location in cylinder	
Type	Ratio, b	On axis	Off axis
Uniform	0.0	2.26	0.0
Uniform	0.2	−8.22	−8.66
Uniform	0.5	−23.94	−20.06
Uniform	1.0	−42.25	−34.98
Non-uniform	0.2	—	8.60

Table 4. Error in calculated activity for an on-axis sphere due to a 6 keV upward shift in the windows. Two background levels are considered. The k value used is that for the standard window with the appropriate background level.

Background ratio, b	Error in calculated activity (%)
0.0	−21.9
0.2	−18.6

Table 5 shows the error with standard windows without scatter correction but with phantom camera calibration. At the lower backgrounds, the absolute value of error with the procedure is quite like that with scatter correction using a universal k value. At $b = 1$, use of a universal k value is more accurate.

Table 5. Percentage activity error without scatter correction using an on-axis sphere in a no-background cylinder as a calibration phantom. Dependence on background and sphere location is given.

Background activity		Hot-sphere location in cylinder	
Type	Ratio, b	On axis	Off axis
Uniform	0	0.0	1.52
Uniform	0.2	9.45	9.98
Uniform	0.5	20.27	23.80
Uniform	1.0	51.55	57.00
Non-uniform	0.2	—	1.20

3.6. Re-evaluation of experimental phantom data

The plot of specific reconstructed count within the geometric VOI versus b is shown in figure 8. The linear fits of the photopeak-window data and the scatter-window data are also shown. The slope, β, and intercept, α, from these plots are quite different from those in the original (figure 3 of the experimental reference). Moreover, the relative ratios are also quite different implying that the k-value dependence on b may now be different.

A list of the calibration factors needed to obtain agreement for the k value between the new experimental results with various-size VOIs and the Monte Carlo results with a geometric volume of interest is given by Luo (1993). An 80% VOI gives the closest agreement with Monte Carlo for the entire background dependence. Figure 6 shows that this agreement is now good.

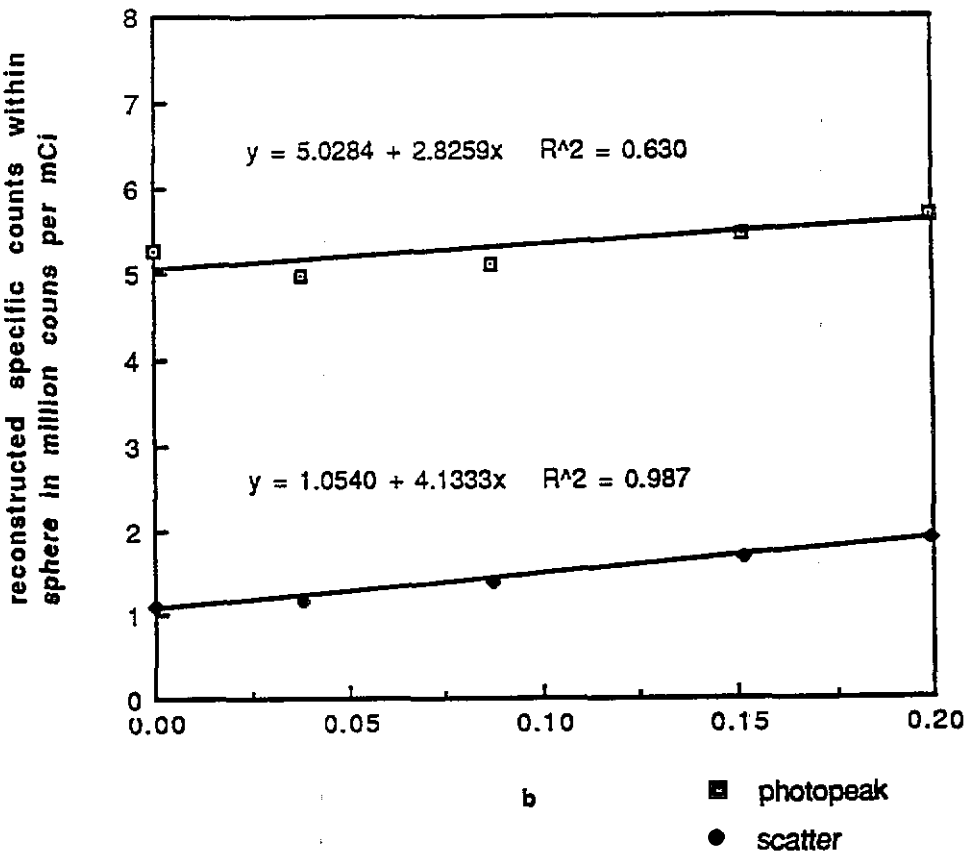

Figure 8. Re-evaluated experimental results for specific reconstructed counts versus b for photopeak and scatter windows. The specific counts are from tomograms of the phantom experiment. Geometric VOI (nominally 5.65 cm diameter). Linear fits to the data are also shown.

4. Discussion

Old experimental results and the Monte Carlo results given here agree as concerns the dependence of the scatter multiplier on cylinder size, sphere location, VOI size, and mode of correction but disagree on the effect of uniform background. However, the formula for evaluating the scatter multiplier experimentally shows that changes in the evaluation of the camera calibration factor can alter the dependence of the multiplier on background. Also, the procedure for carrying out dead-time correction in the experiment has been modified to a more accurate one. Lastly, comparison of the experimental and Monte Carlo results depends on the evaluation of the scale factor (millimetres per pixel) in the experiment. By (1) re-evaluating the experimental data, (2) using an 80%. of nominal geometric VOI, and (3) choosing the unknown camera calibration factor so that the scatter multiplier at zero background is the same as that from Monte Carlo, the entire experimental curve of scatter multiplier versus background essentially agrees with that from Monte Carlo. It appears to us that (1) the experimental data have been reanalysed using a more accurate procedure and

the chosen calibration constant is the true one, (2) the original conclusion that the scatter multiplier is independent of background is wrong, and (3) the dependence is strong as the background increases from zero.

A possible alternative explanation is that there is an experimental procedure which yields little dependence of the scatter multiplier on background. This hypothetical experimental procedure would not remove all effects from scattered counts (Monte Carlo says that a changing value of the scatter multiplier is required to do so), but would somehow compensate for them. Although possible, such an explanation seems unlikely, and the procedure would appear to be hard to duplicate since its characteristics are not completely clear.

Other possibilities are that the Monte Carlo results are in error or that the two approaches (experiment and Monte Carlo) are evaluating significantly different variables. Since we used two separate, independent Monte Carlo programs, we do not think the former is true. As to the latter, it is difficult to see how the variable evaluated could be that different in the two studies.

With respect to quantification, our results show that errors are large if no correction for Compton scattering is carried out while employing a scatter-free camera calibration. On the other hand, scatter correction reduces them if the background is near that employed in determining the universal scatter multiplier. That is, for backgrounds such that b is less than or equal to 0.2, the average absolute value of the error without correction is 22.3%, while that with correction is 5.5%. Here, the universal scatter multiplier is that which is correct at $b = 0.0$. One can compare the active monitoring of a scatter window plus a zero-scatter camera calibration to no scatter correction plus an appropriate, scatter-included camera calibration. Looking only at the comparative results with background as the variable parameter, the two methods are fairly equivalent except at the highest background level ($b = 1.0$). Whether this fact would continue to be true when cylinder size, sphere location, VOI size, and window setting were varied needs further study.

Clinically, background may be enough of a problem for high-accuracy VOI quantification that a multiwindow Compton-scattering correction (Koral *et al* 1988, 1990, Wang and Koral 1992, Ogawa *et al* 1991, Gagnon *et al* 1989) is needed. However, for spectral fitting (Koral *et al* 1988, Wang and Koral 1992) and holospectral imaging (Gagnon *et al* 1989), cameras will have to be changed to yield individual spectra at given camera-face locations. On the other hand, such correction would have the advantage of producing accurate quantitative values throughout the reconstructed volume rather than for only the net reconstructed counts within a spatially limited volume.

An alternative based on the scatter-multiplier method might be to estimate the effective b value for each patient from an initial reconstruction. Then the appropriate k would be chosen from a curve of k versus b. This value would be employed in a final reconstruction to which final VOI quantification would be applied. One would test that the initial effective-background estimate was still approximately correct. If not, further iterations could be carried out. In SP mode, repeat reconstructions would be needed; in ST mode only re-evaluations would be required. The preliminary Monte Carlo phantom results with such a background-adaptive approach are encouraging (Luo and Koral 1994).

We anticipate that the general trends observed with $^{99}Tc^{m}$ will be followed with ^{131}I, an isotope of interest in radiopharmaceutical therapy. Verification of this fact, as well as determination of specific values, however, is needed in future research.

5. Conclusions

The value of the scatter multiplier which produces correct quantification for a radioactive

sphere has only very slight dependence on its location within a cylinder or the cylinder diameter. The scatter multiplier also depends little on whether the correction is before or after the reconstruction. However, the multiplier depends strongly on the level of surrounding uniform background as that background increases from zero. At low background levels, it is sensitive to changes in the size of the volume of interest which is employed, whereas at high background levels it is insensitive. It is unknown whether this insensitivity occurs at very high background levels ($b \gg 1$). Whether the background is uniform, or non-uniform with the same centroid, does not matter.

Activity quantification that ignores scatter correction while using a scatter-free camera calibration yields errors as large as 18.2% even with no background. Quantification is less sensitive to window changes with the scatter-multiplier method than with the split-photopeak correction method (original version).

Quantification with a universal value of the scatter multiplier appears to be fairly accurate (less than 9% error) if the background is reasonably close to that employed in determining the universal value but has much larger error if the background has a large range of values including zero. To avoid error in the second case, a more complex method of correction for Compton scattering is required.

Acknowledgments

The authors thank Steven Buchbinder and Xiaohan Wang for their help in programming. This work was supported by PHS grant number R01 CA38790 awarded by the National Cancer Institute, DHHS and by the Swedish Cancer Foundation, grant 2353-B93-07XAB. Its contents are solely the responsibility of the authors and do not necessarily represent the official views of either the National Cancer Institute or the Swedish Cancer Foundation.

References

Andreo P 1991 Review: Monte Carlo techniques in medical radiation physics *Phys. Med. Biol.* **36** 861–920

Beck J W 1982 Analysis of a camera based single photon emission computed tomography (SPECT) system *Doctoral Dissertation* Duke University

Devito R P, Hamill J J, Treffert J D and Stoub E W 1989 Energy-weighted acquisition of scintigraphic images using finite spatial filters *J. Nucl. Med.* **30** 2029–35

Floyd C E, Jaszczak R J, Harris C C and Coleman R E 1984 Energy and spatial distribution of multiple order Compton scatter in SPECT: a Monte Carlo investigation *Phys. Med. Biol.* **29** 1217–30

Gagnon D, Todd-Pokropek A, Arsenault A and Dupras G 1989 Introduction to holospectral imaging in nuclear medicine for scatter subtraction *IEEE Trans. Med. Imaging* **MI-8** 245–50

Gilardi M C, Bettinarch V, Todd-Pokropek A, Milanesi L and Fazio F 1988 Assessment and comparison of three scatter correction techniques in single photon emission computed tomography *J. Nucl. Med.* **29** 1971–9

Gullberg G T, Huesmant R H, Malko J A, Pelc N J and Budinger T F 1985 An attenuation projector–backprojector for iterative SPECT reconstruction *Phys. Med. Biol.* **30** 799–816

Jaszczak R J, Greer K L, Floyd C E, Harris C C and Coleman R E 1984 Improved SPECT quantification using compensation for scattered photons *J. Nucl. Med.* **25** 983–90

King M A, Hademenos G J and Glick S J 1992 A dual-photopeak-window method for scatter correction *J. Nucl. Med.* **4** 605–12

Knoll G F 1979 *Radiation Detection and Measurement* (New York: Wiley) p 336

Koral K F, Buchbinder S, Clinthorne N H, Rogers W L, Swailem F M and Tsui B M W 1991 Influence of region of interest selection on the scatter multiplier required for quantification in dual-window compton correction *J. Nucl. Med.* **32** 186–7

Koral K F, Swailem F, Buchbinder S, Clinthorne N H, Rogers W L and Tsui B M W 1990 SPECT dual-energy-window Compton correction: scatter multiplier required for quantification *J. Nucl. Med.* **31** 90–8

Koral K F, Wang X, Rogers W L, Clinthorne N H and Wang X 1988 SPECT Compton-scattering correction by analysis of energy spectra *J. Nucl. Med.* **29** 195–202

Koral K F, Zasadny K R, Kessler M L, Luo J, Buchbinder S, Kaminski M S, Francis I and Wahl R L 1994 A method using CT-SPECT fusion plus conjugate views for dosimetry in I-131-MoAb therapy of lymphoma patients *J. Nucl. Med.* **35** 1714–20

Ljungberg M and Strand S E 1989 A Monte Carlo program for the simulation of scintillation camera characteristics *Comput. Methods Prog. Biomed.* **29** 257–72

—— 1990a Comparison of dual window and convolution scatter correction techniques using the Monte Carlo method *Phys. Med. Biol.* **35** 1099–110

—— 1990b Scatter and attenuation correction in SPECT using density maps and Monte Carlo simulated scatter functions *J. Nucl. Med.* **31** 1559–67

Luo J 1993 Dual window scatter correction in quantitative single photon emission computed tomography *Doctoral Dissertation* Oakland University

Luo J and Koral K F 1994 Background-adaptive dual-energy-window correction for Compton scattering in $^{99}Tc^{m}$ SPECT *Nucl. Instrum. Meth. Phys. Res.* at press

Ogawa K, Harata Y, Ichihara T, Kubo A and Hashimoto S 1991 A practical method for position-dependent Compton-scatter correction in single photon emission CT *IEEE Trans. Med. Imaging* **MI-10** 408-12

Raeside D E 1976 Monte Carlo principles and applications *Phys. Med. Biol.* **21** 181

Shepp L A and Vardi Y 1982 Maximum likelihood reconstruction for emission tomography *IEEE Trans. Med. Imaging* **MI-1** 113–32

Wang X and Koral K F 1992 A regularized deconvolution-fitting method for Compton-scatter correction in SPECT *IEEE Trans. Med. Imaging* **MI-11** 351–60

Yanch J C, Flower M A and Webb S 1990 Improved quantification of radionuclide uptake using deconvolution and windowed subtraction techniques for scatter compensation in emission computed tomography *Med. Phys.* **17** 1011–22

Zasadny K R, Koral K F, and Swailem F M 1993 Dead time of an Anger camera in dual-energy-window-acquisition mode *Med. Phys.* **20** 1115–20